Solid State Science and Technology, Vol. 19, No2 (2011) 184-192
ISSN 0128-7389

SILICON NANODOTS GROWN ON SAPPHIRE SUBSTRATE BY A SELF ASSEMBLY GROWTH METHOD

Samsudi Sakrani, Ahmad Radzi Mat Isa and Zulkafli Othaman

Department of Physics, Faculty of Science, Universiti Teknologi Malaysia, 81310 Skudai, Johor, Malaysia

ABSTRACT

Silicon quantum dots have been grown on sapphire substrate using a self-assembly method of physical vapour deposition. The samples were fabricated at low sputtering rate and varying experimental conditions. Apparently, the onset of nucleation took place during the first 5 minutes of deposition, followed by a further growth of stable islands so-called nanodots, with the measured radii comparable to the predicted values. Other measurement results confirmed the existence of these dots, including the bandgap energy ~ 1.80 eV from PL and a 5% at. silicon from EDX. The nucleation parameters were predicted as follows: Free energy change per unit volume $\Delta G_v \sim -2.4 \times 10^5$ Jmol^{-1}; Surface energies per unit area, $\gamma_{LN} = 1.48$ Jm^{-2}, $\gamma_{NS} = 21.6 - 88.3$ Jcm^{-2} and $\gamma_{LS} = 0.82 \times 10^{-2}$ Jm^{-2}; Critical energies $\Delta G^* = 6.83 \times 10^{-16} - 3.68 \times 10^{-14}$ J; Critical radii $r^* = 20 - 72$ nm. This experimental evidence strongly support the early stage growth model of silicon quantum dot deposited on corning glass substrate.

Keywords: Silicon; Self-assembled Growth; Nanodot; Sapphire;

INTRODUCTION

Nanodots, also known as quantum dots, consist of 100s-1000s of atoms of semiconductor nanoparticles and are approximately 10 - 100 nm in sizes. Silicon nanodots have, in particular, emerged over the last 10 years as a hot area of research due to the fact that a reduction in size of this semiconducting material to the nanometer scale dramatically alters their physical properties. Accordingly, nanodots display unique optical and electrical properties that are different in character to those of the corresponding bulk material. The most immediately apparent of these is the emission of photons under excitation, which are visible to the human eye as light. Moreover, the wavelength of these photon emissions depends not on the material from which the nanodot is made, but its size. The smaller the dot, the closer it is to the blue end of the spectrum, and the larger the dot, the closer to the red end. Dots can even be tuned beyond visible light, into the infra-red or into the ultra-violet.

Major applications of silicon nanodots can be found in solid-state lighting devices, mainly for biomedical and optoelectronic applications [1-4]. Luminescent silicon quantum dots have great potential for use in biological imaging and sensors [5]. Other application of this novel material is in the field of silicon thin film solar cells. A combined nc-Si and a-Si layers is possible, creating a layered, multi-junction cell called

Solid State Science and Technology, Vol. 19, No2 (2011) 184-192
ISSN 0128-7389

a tandem cell. The top cell in a-Si absorbs the visible light and leaves the infrared part of the spectrum for the bottom cell in nanocrystalline Si [6].

NUCLEATION AND GROWTH THEORY

From the well known growth mechanisms [7] a particular attention is given on the island's Volmer-Weber (V-W) growth shown in Figure 1 where the contribution of surface parameters are very significant if compared to that of misfits at the material-substrate interface. Most amorphous and non-crystalline semiconductors appeared to fulfill the growth conditions.

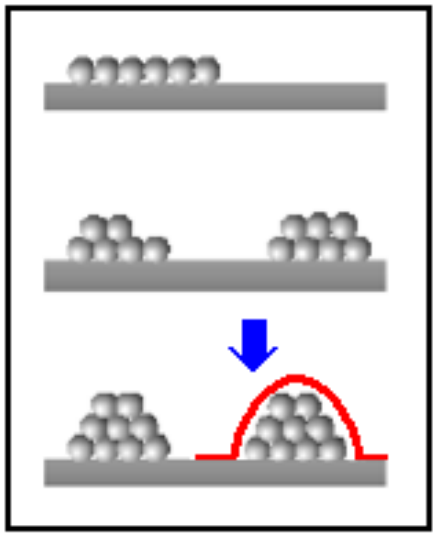

Figure 1: Volmer-Weber growth mode

When a liquid is transformed into a solid phase the transition is often initiated by a nucleation process, manifested by the appearance of nuclei of the new phase. The process is made possible by diffusion of atoms or molecules that aggregate to form the nuclei of liquid, with the size of these nuclei increases with time and at the end of the process a new homogenous solid is formed, i.e. 3-dimensional islands with increased volume. Bauer (1980s) was the earliest to describe thin film growth in terms of surface energy with the relation: $\gamma_{film} \leq \gamma_{substrate} - \gamma_{interface}$. Under the V-W growth mode, a stable nucleus is governed by three surface energies per unit area, γ_{LS}, γ_{LN} and γ_{NS} and contact angle, θ according to the relationship, $\gamma_{LS} \leq \gamma_{LN} cos\theta + \gamma_{NS}$. Under the condition of -1 < $\cos\theta$ < 0 (for θ > 90°) an oval shaped nanodot is formed, with atoms of the nucleus bonded to each other. This non-wetting condition remains stable if $\gamma_{LN}\cos\theta + \gamma_{NS}$ is kept in higher value than γ_{LS}. The experimentally-observed oval shape nanodots can be further studied in order to give information on various parameters involved. Based on this theory silicon nanodot is expected to be formed on saphire substrates, and it is the purpose of our investigation to look into how self-assembled growth is taking place.

Solid State Science and Technology, Vol. 19, No2 (2011) 184-192
ISSN 0128-7389

HIGH TEMPERATURE NUCLEATION

The classical theory of heterogeneous nucleation treats the forming nucleus as part of a sphere attached to the substrate, which is different from a spherical droplet considered for homogeneous nucleation. Fig. 1 shows a typical shape of nucleus which is capped in red, known in different names such as, cap, dome, inverted bowl-shaped. This nucleus is thought to consist of incompressible, uniform liquid/solid and a part of a sphere with the base attached to the insoluble surface. There are interfaces between the solid nucleus-substrate surface, liquid-solid nucleus and liquid-substrate surface, each of which is shown by the respective surface energies per unit area, γ_{NS}, γ_{LS}, and γ_{LN}. The angle θ between the nucleus surface and the substrate surface is called the contact angle. The critical radius in heterogeneous nucleation is the same as in homogeneous nucleation, as it only depends on ΔG_v (change in energy of solidification). The substrate surface is usually considered homogeneous, although there is a possibility of some non-uniform surfaces. In this investigation planar substrate surface geometry is treated.

From the thermodynamic point of view, a change in the free enthalphy, ΔG is associated with nucleation via the following four processes: Firstly, creation of new volume of the nucleus (negative); secondly existence of surface area of liquid-nucleus (positive), thirdly existence of surface area of liquid-nucleus (positive) and lastly the energy lost at liquid-substrate interface (positive). Thus [8],[9],

$$\Delta G = \alpha_3 r^3 L_f \frac{\Delta T}{T_m} + \alpha_1 r^2 \gamma_{LN} + \alpha_2 r^2 \gamma_{NS} - \alpha_2 r^2 \gamma_{LS} \qquad (1)$$

where, $\alpha_1 = 2\pi(1-\cos\theta)$, $\alpha_2 = \pi\sin^2\theta$, $\alpha_3 = \pi(2-3\cos\theta+\cos^3\theta)/3$, $\Delta G_v = L_f(\Delta T/T_f)$ is the energy change per unit area of the nucleus and has the values depending on the undercooling temperature, ΔT (T_m-T); positive if $T > T_m$, with T_m being the temperature of the transition (solidification temperature), L_f is entalphy of fusion. Under these conditions, applying the Gibbs-Duhem principle, the new phase is not stable. Since γ is a positive quantity, ΔG_v is then positive: the number of nuclei of the new phase are not stable and do not tend to grow. On the contrary, if $T < T_m$, is negative, the new phase (solid) is stable. There are values of r for which $\Delta G_v < 0$, and the corresponding nuclei will tend to stabilize the new phase since their formation reduces the free enthalpy of material. When $T < T_m$ ($\Delta T > 0$), ΔG_v has a maximum for $r = r^*$. For $r > r^*$, the formation of nuclei of increasing size can results in stabilization of the solid phase since ΔG_v decreases and even becomes negative. Both the critical energy, ΔG^* and critical radius, r^* are obtained as,

$$\Delta G^* = \frac{16\pi\gamma_{NS}^3 T_m^2}{3L_f^2 \Delta T^2}\left(\frac{2-3\cos\theta+\cos^3\theta}{4}\right) \qquad (2)$$

Solid State Science and Technology, Vol. 19, No2 (2011) 184-192
ISSN 0128-7389

$$r^* = \frac{-2\gamma_{NS}}{\Delta G_v} = \frac{-2\gamma_{NS} T_m^2}{L_f^2 \Delta T^2} \qquad (3)$$

ΔG^* is equivalent to the potential barrier that must be lowered for nuclei of critical size r^* to be formed more easily. It seems that from equation (1) the more important supercooling is, the more this barrier is lowered. The Volmer thermodynamic model shows that a complete phase transition by nucleation is only possible if the liquid is supercooled. In fact, nucleation is initiated with lower *supercooling* (larger ΔT) because the impurities present in the liquid phase, even in low concentration, induce nucleation, normally referred to heterogeneous nucleation.

EXPERIMENTAL DETAILS

The samples were fabricated using a magnetron sputtering system at reasonbly low deposition rate of 2.7×10^{-2} nms^{-1} and varying experimental conditions: Chamber pressure of 10^{-2} Torr, heater temperature 100-400°C, fixed argon flow rate 5 sccm, and deposition times varied between 5–20 minutes. The principal process was based on high energetic burial of target materials previously removed by positive ion bombardment within the plasma region. This high-speed particle transportation may contributes to the initial growth of quantum dot on selected substrate surface. The samples were analysed using photoluminescence, EDX and XRD. A theoretical investigation was done using the classical approach of heterogeneous nucleation in which the net energy change required to form a spherical nucleus is equivalent to the summation of energy terms associated with four different interfacial interactions.

RESULTS AND DISCUSSION

The analysis obtained from AFM (Figures 2 and 3) shows that the sample fabricated at 5 minutes after deposition, temperature 400 °C and power 100W is comprised of smaller dots, whilst that of 5 mins/400 °C/100W containing bigger sizes. The onset of dot's growth appears to be 30 mins after the deposition that grows laterally and vertically until stable dome-like shapes are finally formed. Further analysis on the cross sectional area reveals the dot's sizes between 40 – 155 nm in diameter. This hat-like appearance is slightly contrary to a dome-like shape predicted from the theory. For the nanodots fabricated at temperatures less than 400 °C the observed appearance is very weak or inexistence of the dot formation. The dependence of contact angle, θ at 70° was found to be less significant as can be observed for the case of r^* (not shown in graph). Some selected samples were analyzed using photoluminescence (PL) and XRD in order to determine the band gap energy, E_g and contents, respectively. From PL spectrum shown in Figure 4, E_g were found to be ~1.8 eV, a value which is greater than that of bulk silicon (> 1.1 eV). This result is also supported by the EDX analysis for 400 °C/100W samples (Figure 5) which reveals 5% of atomic Si in the sample. All the above results confirm the existence of Si nanodot.

Solid State Science and Technology, Vol. 19, No2 (2011) 184-192
ISSN 0128-7389

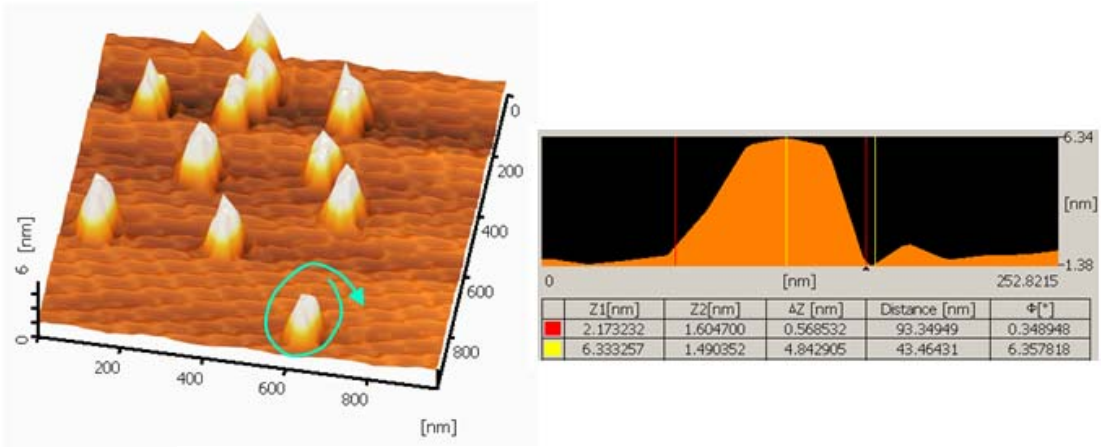

Figure 2: AFM image of Si nanodots: 3 mins/100 W/400 °C

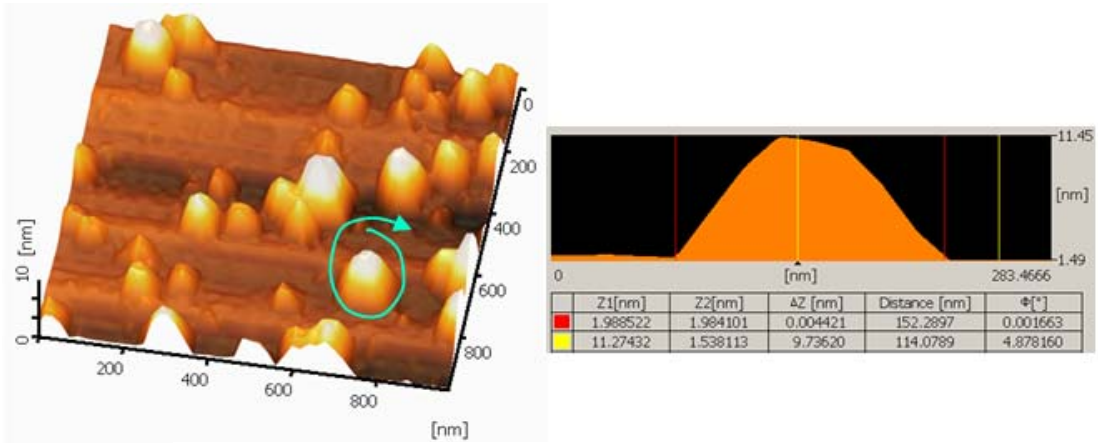

Figure 3: AFM image of Si nanodots: 10 mins/100 W/400°C

Simulation works have been done based on the classic nucleation theory given by equations (1) to (3). A computer program was written using a visual basic to include the following parameters: Enthalpy of fusion, L_f = 3.96 x 10^4/mol; melting temperature of silicon, T_m = 1683 K; substrate temperature, each for T = 673 K; undercooling temperature, each for T_m-T = 1110 K dan 1010 K respectively, atomic volume, v_o = 12.1 cm^3/mol and contact angle, θ = 70°. The simulation results have been obtained and are shown in Table 1.

Solid State Science and Technology, Vol. 19, No2 (2011) 184-192
ISSN 0128-7389

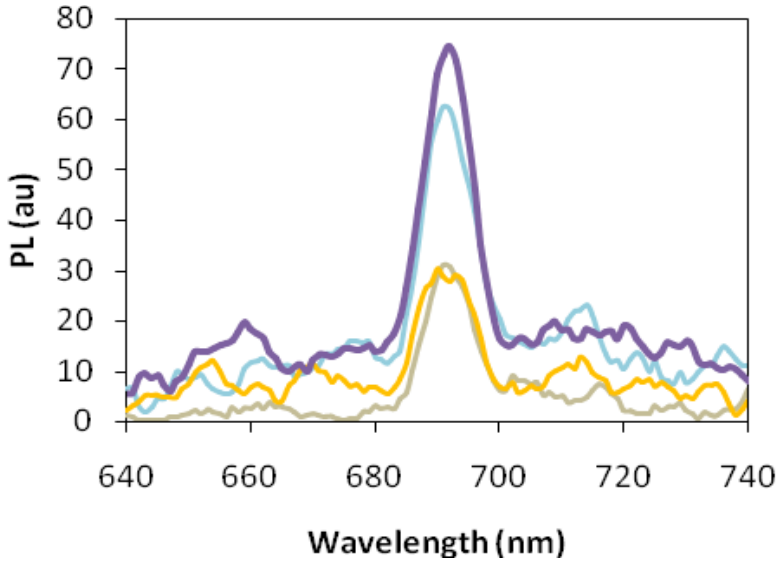

Figure 4: PL spectrum of nanodots

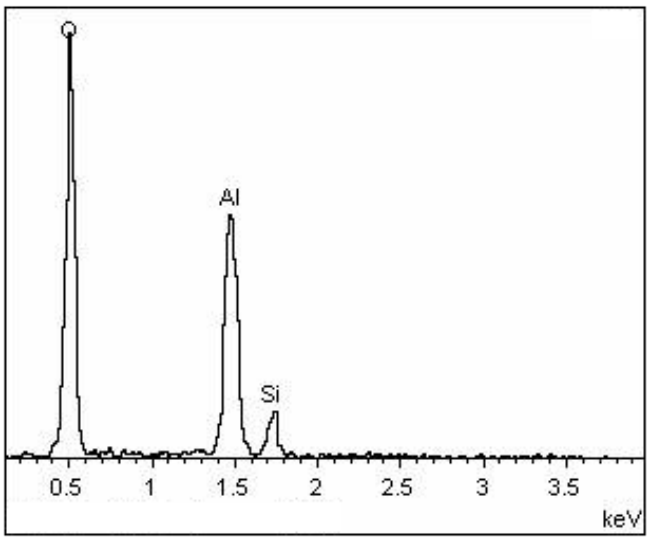

Figure 5: EDX results showing a weak Si peak

Solid State Science and Technology, Vol. 19, No2 (2011) 184-192
ISSN 0128-7389

Table 1: Experimental and simulation data

Experimental	T=573K	Simulation	γ_{LN} =1.48 x 10^{-4} Jcm^{-2}	γ_{LS} =8.2 x 10^{-5} Jcm^{-2}
d (nm)	r^*(nm) = $d/2$	γ_{NS} (Jcm^{-2})	r^*(cm)	ΔG^*(J)
40.5	20.1	21.6 x 10^{-4}	2.03 x 10^{-6}	6.83 x 10^{-16}
56.2	28.4	30.3 x 10^{-4}	2.81 x 10^{-6}	1.79 x 10^{-15}
93.3	46.5	51.3 x 10^{-4}	4.67 x 10^{-6}	8.25 x 10^{-15}
117.4	58.4	64.8 x 10^{-4}	5.87 x 10^{-6}	1.63 x 10^{-14}
135.8	68.2	75.2 x 10^{-4}	6.79 x 10^{-6}	2.54 x 10^{-14}
153.6	76.8	85.3 x 10^{-4}	7.68 x 10^{-6}	3.68 x 10^{-14}

Figures 6 and 7 show the variations of ΔG^* and r^* with γ_{NS} for T=673 K. The graphs clearly indicate increasing trends shown by the linear and curvy variations, respectively as predicted from the theory. There are also points on the graphs indicating the measured values of r^* ranging between 20-77 nm (not shown) corresponding to nanodot's sizes of 40-154 nm. These results strongly suggest that both critical parameters are the functions of surface energy at the nucleus-surface interface and contact angle between the nucleus and substrate.

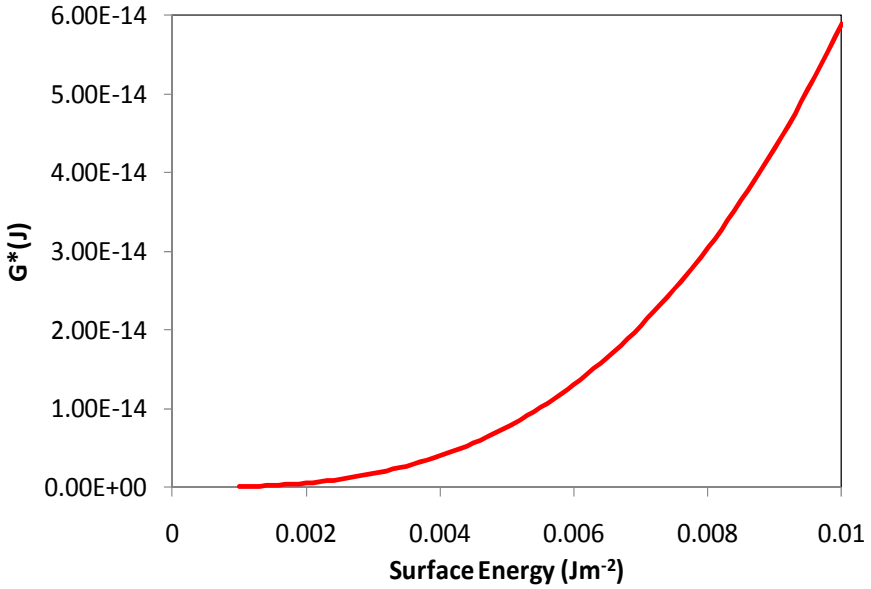

Figure 6: Critical energy, ΔG^* versus surface energy, γ_{NS}

Solid State Science and Technology, Vol. 19, No2 (2011) 184-192
ISSN 0128-7389

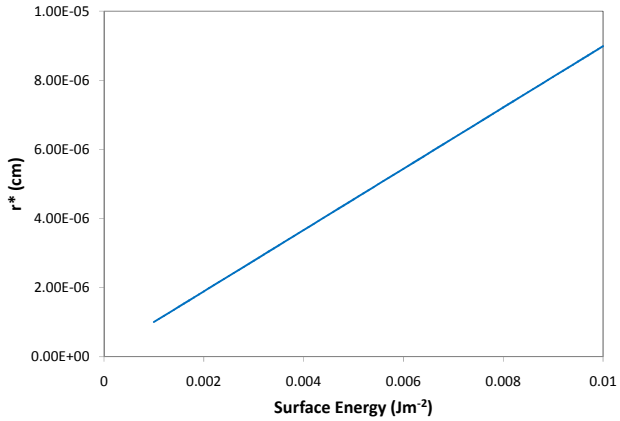

Figure 7: Critical radius, r^* versus surface energy, γ_{NS}

It is observed that, from the above results the growth of silicon nanodot satisfies equation (1), under the condition of $\gamma_{LN}\cos\theta + \gamma_{NS}$ which exceeding or greater than γ_{LS}. An example of simulated parameters for T = 673 K is tabulated in Table 1, together with the measured diameters and r^*. It is important to note that, there is a very good compromise between the theoretical and experimental data, mainly the value silicon surface energy, γ_{LN} =1.48 x 10^{-4} Jcm^{-2} [10],[11].

CONCLUSION

The self-assembled growth of silicon nanodots can be well described using the Volmer-Weber growth mode mechanism, based on the non-wetting oval shape cluster. Slight modifications of this oval to dome-like shape are needed in order to satisfy the liquid-solid nucleation theory. Accordingly, the sums of $\gamma_{LN}\cos\theta + \gamma_{NS}$ are just reasonably greater than $\gamma_{LS,}$ and these have been verified experimentally. The self-assembly method can be applied for the fabrication of quantum devices, such as quantum dot single-electron transistor and nanobiosensor.

ACKNOWLEDGEMENT

The authors would like to thank the Ministry of Higher Education, Malaysia for providing financial support under the FRGS grant (Vot No. 78461).

REFERENCES

[1] P. N. Prasad, Introduction to Biophotonics. (Wiley-Interscience; Hoboken, New Jersey 2003)
[2] X. Gao, L. Yang, J. A. Petros, F. F. Marshall, J. W. Simons and S. Nie, *Current Opinion in Biotechnology*, **16** (2005) 63–72
[3] I. L. Medintz, H. T. Uyeda, E. R. Goldman, H. Mattoussi, *Nat Mater.*, **4** (2005) 435–446
[4] J. P. Wolfgang, P. Teresa, P. Christia, *Nanotechnology*, **16** (2005) R9-R25
[5] A. Cavalcanti, B. Shirinzadeh, M. Zhang, L. C. Kretly, *Sensors* **8** (5) (2008) 2932–2958
[6] D. Crisp, A. Pathareb and R. C. Ewell, *Progress in Photovoltaics Research and Applications*, **54** (2) (2004) 83–101
[7] I Daruka and A-L. Barabasi, *Physical Review Letters*, **79** (19) (1997) 3708-3711
[8] S. Sakrani, Q. J. Lim and Y. Wahab, *J. Fundamental Sciences*, **3** (1) (2007) 158-165
[9] S. Sakrani, Q. J. Lim and Y. Wahab, *J. Fundamental Sciences*, **1** (1) (2005) 21-31
[10] I. Satoshi, H. Shotaro and S. Shinsuke, *J. of the Society of Materials Science (Japan)*, **52** (2003) 231-234
[11] R. R. Tummala and B. J. Foster, *J. Mat. Science*, **10** (5) (1975) 1575-4803